Biological effect of ribosomal protein L32 on human breast cancer cell behavior

LU XU[1*], LINTAO WANG[2*], CHAOJUN JIANG[3], QIANNAN ZHU[3], RUI CHEN[3], JUE WANG[3] and SHUI WANG[3]

[1]Clinical Nutrition Department, The First Affiliated Hospital of Nanjing Medical University; [2]Department of Biochemistry and Molecular Biology, Nanjing Medical University; [3]Breast Disease Department, The First Affiliated Hospital of Nanjing Medical University, Nanjing, Jiangsu 210000, P.R. China

Received July 13, 2019; Accepted June 4, 2020

DOI: 10.3892/mmr.2020.11302

Abstract. Breast cancer (BC) is the most common malignancy among women worldwide. However, identifying effective biomarkers for the diagnosis and treatment of BC is challenging. Based on our previously developed 'humanized' mouse model of BC, microarray expression analysis was performed and multiple differentially expressed genes, including ribosomal protein (RP) L32, were screened. Recent reports have revealed that RPs are relevant to the development and progression of cancer. However, the expression and function of RPL32 in BC remains unknown. Therefore, in the present study, the role of RPL32 in the development of BC was explored. Immunohistochemical staining and reverse transcription-quantitative PCR were used, and it was found that RPL32 was upregulated in human BC tissues and cells. Cell Counting Kit-8, cell invasion and migration assays were performed, which demonstrated that RPL32 knockdown using lentivirus-delivered small interfering RNA inhibited the migration and invasion of BC cells *in vitro* and *in vivo* (nude mouse model). Moreover, western blotting showed that RPL32 knockdown decreased the expression levels of matrix metalloproteinase (MMP)-2 and MMP-9. Thus, the present findings indicated a potential oncogenic role of RPL32, suggesting that it may be a novel target for molecular targeted therapy in patients with BC.

Correspondence to: Professor Jue Wang or Professor Shui Wang, Breast Disease Department, The First Affiliated Hospital of Nanjing Medical University, 300 Guangzhou Road, Nanjing, Jiangsu 210000, P.R. China
E-mail: wangjue200011@njmu.edu.cn
E-mail: ws0801@hotmail.com

*Contributed equally

Key words: ribosomal protein L32, breast cancer, migration, invasion

Introduction

Breast cancer (BC) is currently the most common cancer type worldwide. For instance, according to the 2015 World Health Organization World Cancer Report, there are ~14,000,000 new cases and 8,200,000 BC-related mortalities worldwide (1). Over the last few decades in China, the incidence of BC has increased and account for 15% of all new cancer cases in women. The age of onset has decreased and breast cancer is the most diagnosed cancer between the ages of 30 and 59 years old (2,3). Despite the significant achievements in BC therapy, as a result of developments in modern technology, the precise molecular mechanisms underlying the progression of BC remain unknown (4,5). Therefore, the identification of biomarkers is required for a more effective diagnosis and treatment of BC.

A previous study (6) developed a humanized mouse model of BC, in which healthy human breast tissues were implanted into the flank of the mice. Human BC cells were then injected into the implanted human breast tissues, and the results of this study revealed that human BC cells proliferate well in human breast tissues and metastasize into distantly implanted human tissues (6). Moreover, human BC cells obtained via primary culture from the primary human BC lesion in the mouse model, demonstrate a more aggressive behavior *in vitro* (7). In another previous study, microarray expression analysis was performed and multiple differentially expressed genes were screened, including ribosomal protein (RP) L32 (8). RPL32 encodes an RP that is a component of the 60S subunit. Furthermore, this protein belongs to the L32E family of RPs and is located in the cytoplasm.

RPs are components of ribosomes involved in protein translation and ribosome assembly (9). According to the size of the subunits they are derive from, RPs are termed large or small subunit RPs. However, it has been revealed that certain RPs are expressed in tissue-specific patterns and can differentially contribute to ribosome composition, affect ribosomal RNA processing and regulate translation (10). Previous studies have reported that perturbations of several individual RPs occur in numerous types of human cancer, including cancer of the brain, pancreas, bladder and other tissues (11-17). These studies have rapidly established mutations in RPs as a novel, underexplored class of oncogenic factors. For example, it has been shown that

the expression of RPL22 is significantly downregulated at the mRNA and protein level in non-small cell lung cancer (18). Furthermore, RPL31 modulates prostate cancer cell proliferation via the p53 pathway (19). RPS15A also promotes malignant transformation and predicts the outcome of colorectal cancer via the misregulation of the p53 signaling pathway (20).

In the present study, the expression of RPL32, whose biological and clinical significance is yet to be elucidated, was evaluated in human breast tumor tissues, the SUM 1315 human BC line and an *in vivo* mouse model.

Materials and methods

Cell culture. MCF-10A human breast epithelial and BT474, MDA-MB-231 and HCC-1937 human BC cell lines were obtained from the American Type Culture Collection. The human BC SUM 1315 cell line, an estrogen receptor-, progestogen- and human epidermal growth factor receptor 2-negative BC cell line, was provided by Dr Stephen Ethier (University of Michigan). The cells were cultured in a humidified atmosphere of 5% CO_2 at 37˚C and with complete high glucose DMEM (Wisent Biotechnology), supplemented with 10% FBS (Wisent Biotechnology), 100 U/ml penicillin and 100 μg/ml streptomycin (Beyotime Institute of Biotechnology).

Transfection of green fluorescent protein (GFP). SUM 1315 cells were grown in a 6-well cell culture cluster. When cells reached ~80% confluence, the culture medium was removed, and 2 ml plenti-GFP lentivirus (provided by Professor Beicheng Sun, Nanjing Drum Tower Hospital, the Affiliated Hospital of Nanjing University Medical School, Jiangsu, China) combined with 12 μl polybrene (Sigma-Aldrich; Merck KGaA) were added. After incubation for 4 h, 2 ml culture medium was added. After 24 h, the mixed medium was replaced by the fresh culture medium for further culturing and passaging.

Tissue microarray and immunohistochemical staining. The microarray of BC tissue (all from female patients with BC), which contained 128 samples of infiltrating ductal carcinoma and six samples of infiltrating ductal carcinoma with infiltrating lobular carcinoma (HBre-Duc150-Sur-01), was purchased from Outdo Biotech Co., Ltd. The mean age of patients was 53.3±13.2 years old and the mean tumor size was 3.4±1.8 cm. A total of 11 patients had tumor Grade I, 47 tumor Grade II and 76 tumor Grade III (according to 7th Tumor, Node, Metastasis staging system; American Joint Committee on Cancer). A total of eight patients were clinical Stage I BC, 80 clinical Stage II and 46 clinical Stage III. The patients whose samples were included in the microarray underwent surgery between January 2001 and August 2004 in local hospitals.

Tissue microarray sections (thickness, 5 μm) were dewaxed and the endogenous peroxidase was quenched with 3% H_2O_2 in methanol for 30 min at room temperature. Prior to staining, non-specific binding was blocked by incubation with 10% BSA (Beijing Solarbio Science & Technology Co., Ltd.) in PBS at 37˚C for 1 h. Tissue sections were incubated with a primary antibody against RPL32 (1:1,000, cat. no. ab229758; Abcam) in PBS containing 1% BSA at 4˚C overnight, followed by incubation with horseradish peroxidase (HRP)-conjugated anti-rabbit (1:500) or anti-mouse (1:500) antibodies (cat. nos. BS13278 or BS12478; Bioworld Technology, Inc.) for 1 h at room temperature. The color was then developed by incubation with an ImmunoPure Metal Enhanced Diaminobenzidine Substrate kit (Thermo Fisher Scientific, Inc.). Following incubation, the tissue sections were washed three times with PBS for 10 min. The tissue sections were finally counterstained with 1% hematoxylin for 5 min at room temperature.

To determine the expression of RPL32, cytosolic staining of yellowish or brownish granules was graded as follows: i) 0, background staining; ii) 1, faint staining; iii) 2, moderate staining; and iv) 3, strong staining. In addition, positive staining areas in entire tissue sections were graded as follows: i) 0, <5%; ii) 1, 5-25%; iii) 2, 26-50%; iv) 3, 51-75%; and v) 4, 76-100%. Combining these two parameters, 0-2 and ≥3 were defined as negative and positive staining, respectively. The stained tissue microarray samples were assessed using an ECLIPSE microscope (Nikon Corporation) and scored with a semi-quantitative scale by two independent blinded investigators.

Cell transfection. The commercial lentiviral construct LV3-RPL32-siRNA vector (RPL32 siRNA; GeneChem, Inc.) was modified to knockdown RPL32 (target sequence, 5'-CTC ACAATGTTTCCTCCAA-3') in the SUM 1315 human BC lines. The LV3 empty construct (control siRNA) served as the negative control. SUM 1315 cells stably transfected with the negative control were termed '1315-CON' and those subjected to RPL32 knockdown were '1315-KD'. Cells were plated in 6-well plates at 30-40% confluence and infected with the lentivirus, according to the manufacturer's instructions. Polybrene (5 μg/ml; Sigma-Aldrich; Merck KGaA) was added to the lentivirus to enhance the infection efficiency. Stable pooled populations of BC cells were generated using puromycin (3 μg/ml) for 2 weeks. Then, RPL32 expression was analyzed using reverse transcription-quantitative (RT-q)PCR and western blotting.

RT-qPCR. Total RNA was isolated from tissues using TRIzol® reagent (Invitrogen; Thermo Fisher Scientific, Inc.) and cDNA was synthesized using PrimeScript RT reagent (Takara Bio, Inc.), following the manufacturer's instructions. The PCR amplification conditions used were 94˚C for 30 sec, 35 cycles of 94˚C for 30 sec, 55˚C for 30 sec and 72˚C for 1 min, followed by 72˚C for 10 min. β-actin (ATCB) was used as the endogenous reference gene. The following PCR primers were used: ATCB forward, 5'-GCTGTGCTATCCCTGTACGC-3' and reverse, 5'-TGCCTCAGGGCAGCGGAACC-3'; and RPL32 forward, 5'-CTGGTCCACAACGTCAAGGAG-3' and reverse, 5'-CACGATGGCTTTGCGGTTC-3'.

All PCR reactions were performed using the fluorescent SYBR-Green I methodology. RT-qPCR was performed using a StepOnePlus RT PCR system (Thermo Fisher Scientific, Inc.) using FastStart Universal SYBR Green Master (Roche Diagnostics), according to the manufacturer's instructions. The RT-qPCR conditions consisted of an initial denaturation step at 95˚C for 10 min, followed by 40 cycles of 15 sec at 95˚C and 1 min at 60˚C. A melting curve was set at 95˚C for 15 sec, 60˚C for 15 sec and 95˚C for 15 sec at the end of each run to

verify the specificity. Relative quantification was calculated using the $2^{-\Delta\Delta Cq}$ method (21) and normalized based on the expression of ACTB.

Western blotting. Cells were scraped from the plates (cell density 80-90%), rinsed with ice-cold PBS and lysed in cell lysis buffer containing protease and phosphatase inhibitors to obtain total protein extracts (cat. no. P0013C; Beyotime Institute of Biotechnology). The protein concentrations were determined using a bicinchoninic acid protein assay (Thermo Fisher Scientific, Inc.) and equal amounts of protein (60 μg) were separated using SDS-PAGE and transferred to polyvinylidene fluoride membranes. The percentage of SDS-PAGE for RPL32, matrix metalloproteinase (MMP)-2 and MMP-9 was 12, 10 and 10%, respectively. The membranes were then blocked with 5% non-fat milk at room temperature for 2 h. Following which, membranes were washed three times with TBS buffer with 0.1% Tween-20 and then incubated with the following primary antibodies overnight at 4˚C: Anti-RPL32 (cat. no. ab229758; Abcam), anti-MMP-2 (cat. no. ab92536; Abcam), anti-MMP-9 (cat. no. ab38898; Abcam), anti-β-actin (cat. no. BS1002; Bioworld Technology, Inc.) and anti-GAPDH (cat. no. AP0063; Bioworld Technology, Inc.). Then, membranes were incubated with HRP-conjugated secondary anti-rabbit (1:2,000, cat. no. BS13278; Bioworld Technology, Inc.) and anti-mouse antibodies (1:2,000, cat. no. BS12478; Bioworld Technology, Inc.) for 1 h at room temperature. The antibodies were diluted according to the manufacturer's instructions. Immunoreactive proteins were visualized using the SuperSignal West Femto Maximum Sensitivity Substrate kit (Thermo Fisher Scientific, Inc.). The signals were detected using FluorChem E System (ProteinSimple). The density of each band was quantified using Photoshop CC 2017 release (Adobe Systems, Inc.) and plotted using GraphPad Prism 5 (GraphPad Software, Inc.). The levels of the proteins were normalized to those of the corresponding total protein; the levels of all the other targeted proteins were normalized to those of GAPDH and β-actin.

Cell Counting Kit (CCK)-8 cell viability assay. Cell viability was assessed using a CCK-8 (Dojindo Molecular Technologies, Inc.), according to the manufacturer's instructions. Cells ($3x10^3$/well) were seeded into 96-well plates and cultured overnight. At 0, 24, 48 and 72 h, the CCK-8 reagent (10 μl) was added to each well and incubated at 37˚C for 1 h. The absorbance was then measured at 450 nm (optical density value) using an automated microplate reader (Tecan Group, Ltd.) Each experiment was performed ≥3 times independently.

Cell invasion and migration assays. Cells that were to be tested for invasion were collected by trypsinization, washed with PBS, resuspended in conditioned medium and then added to the upper chamber of Matrigel-coated (precoating at 37˚C for 30 min) invasion filter inserts (8-μm pore size) at $5x10^4$ cells/well. Conditioned medium without serum (600 μl) was plated into the lower compartment of the invasion chamber. The chambers were incubated at 37˚C for 24 h in 5% CO_2. Following incubation, the filter inserts were removed from the wells and the cells on the upper side of the filter were removed mechanically by wiping, using a cotton swab. The filters were fixed for 10 min with 4% paraformaldehyde and stained with 1% hematoxylin and eosin for 10 min at room temperature. The cells invading through the Matrigel were located on the underside of the filter. Images of three random fields were captured with a fluorescent microscope (LSM710) at magnification x100, and the number of cells was counted to calculate the mean number of cells per field that had transmigrated.

Cells ($5x10^5$) were seeded in 6-well plates and grown to 90% confluence in 2 ml growth medium. The cells were carefully wounded using a 5-mm-wide tip and cellular debris was removed by washing with DMEM. The cells were cultured in DMEM serum-free medium. Cell migration into the wound area was imaged at the indicated time points (0 and 48 h) with a fluorescent microscope (LSM710) at magnification x100, and analyzed by ImageJ software (v1.8.0; National Institutes of Health).

Animal model construction. All procedures involving mice and the corresponding experimental protocols were approved by the Animal Care and Use Committee of Nanjing Medical University (approval no. IACUC-1706010). A total of 18 female nude mice (BALB/c Nude; age, 4-5-weeks; body weight ~14-16 g) were purchased from the Model Animal Research Center of Nanjing University and randomly divided into two groups (1315-CON and 1315-KD, n=9 mice/group). Randomization was created using the standard=RAND() function in Microsoft Excel (Office 2016 edition). Mice were housed in groups of 4-5. Environmental conditions in the animal lab (Nanjing Medical University) were a temperature of 21˚C, humidity of 55% and under specific pathogen free conditions. Cages ($330x205x130$ mm^3), bedding and drinking water were autoclaved and changed regularly. Food was sterilized by irradiation. Food and water were available *ad libitum*. The mice were maintained in a 12-h light/dark cycle. During housing, animals were monitored daily for health status.

Mice were anesthetized by intraperitoneal injection with pentobarbital sodium (40 mg/kg body weight; Sigma Fenstertechnik GmbH & Co.). Each group received a subcutaneous injection of $5x10^5$ 1315-CON or 1315-KD cells into the mammary fat pad. Tumor size and animal weight were measured every 2 days. Prior to sacrifice, the orthotopic tumor mass of mice was measured in two dimensions with calipers and the tumor volume was calculated according to the equation (length x width x width)/2. After 28 days, all the mice were sacrificed by intraperitoneal injection with pentobarbital sodium (100 mg/kg body weight). The mouse death was verified 10 min after injection, for ≥5 min using the following criteria: i) No breath; ii) no heartbeat; iii) no nerve reflexes; and iv) muscles relaxed. The primary endpoint were the incidence of tumor formation and metastases. The criteria for determining the time of mouse euthanized included: i) Body weight loss >20%; ii) loss of appetite for 24 h; iii) the food intake decreased to half; iv) too weak to stand; v) infection; and vi) low body temperature.

Statistical analysis. All the data for the different experimental groups are presented as the mean ± SD, and were obtained from ≥3 independent experiments. The statistical analysis was performed using SPSS version 19.0 (IBM Corp.). The gray

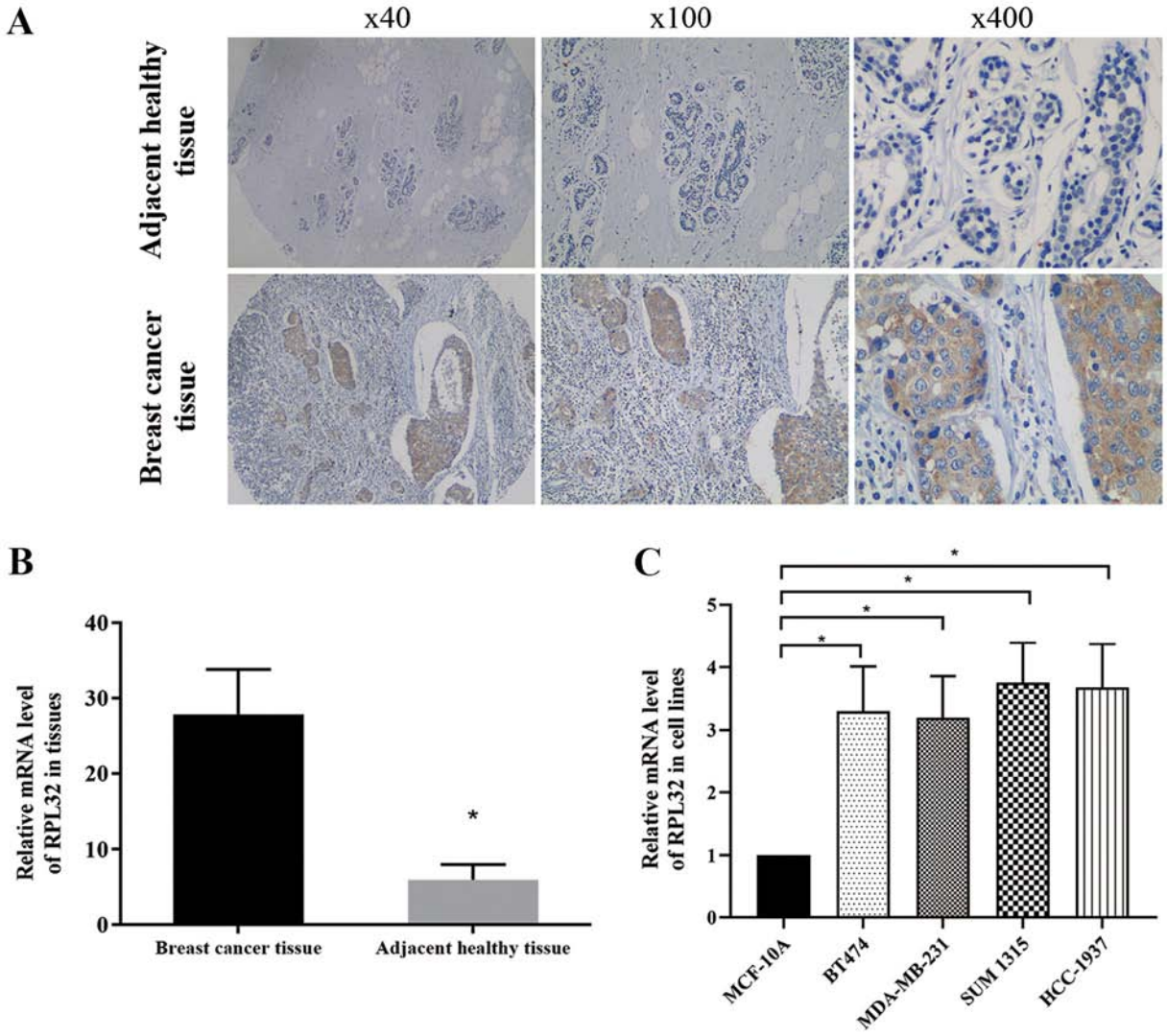

Figure 1. RPL32 is upregulated in BC tissues. (A) A pronounced immunohistochemical staining of RPL32 was detected in BC specimens compared with matched healthy tissues. (B) A higher mRNA expression of RPL32 was detected in BC compared with adjacent healthy breast tissues, as determined by RT-qPCR. (C) A higher mRNA expression of RPL32 was detected in BC cell lines compared with the normal breast epithelial cell line, as determined by RT-qPCR. *P<0.05 vs. breast cancer tissue or MCF-10A cells. RPL32, ribosomal protein L32; BC, breast cancer; RT-qPCR, reverse transcription-quantitative PCR.

values of protein bands on the western blots (mean ± SD) were normalized to those of GADPH or b-actin, and compared using an unpaired Student's t-test. All *in vitro* experiments were performed in triplicate. Differences between each group *in vitro* were analyzed using Student's t-tests and one-way ANOVA followed by Dunnett's post hoc test. P<0.05 was considered to indicate a statistically significant difference.

Results

RPL32 is upregulated in BC. Immunohistochemical staining was used to assess the RPL32 expression in 134 pairs of BC and matched adjacent healthy tissues. The results demonstrated strong RPL32 staining in most BC specimens and a weak staining in matched healthy tissues (Fig. 1A). RT-qPCR was then used to detect the relative mRNA expression of RPL32 in BC and matched adjacent healthy tissues, and the results were consistent with those of the immunohistochemical assay (Fig. 1B).

RT-qPCR was also used to compare the RPL32 gene expression among breast epithelial and BC cell lines. It was identified that RPL32 expression significantly higher in BC cell lines compared with the normal breast epithelial cell line (Fig. 1C).

Lentivirus-delivered siRNA silencing specifically inhibits the expression of RPL32 at the mRNA and protein levels. To study the role of RPL32 in BC, lentivirus-delivered siRNA targeting RPL32 was used in SUM 1315 cells. RPL32 and control siRNAs were constructed. The infection efficiency of the lentivirus was assessed by detecting the GFP expression 3 days after transduction. As presented in Fig. 2A, >90% of the cells were infected. In addition, RT-qPCR and western blotting were used to analyze the knockdown efficiency of RPL32 in SUM 1315 cells. It was demonstrated that RPL32 mRNA expression was reduced by ~90% following RPL32 silencing compared with the 1315-CON group (Fig. 2B). The RPL32 protein expression

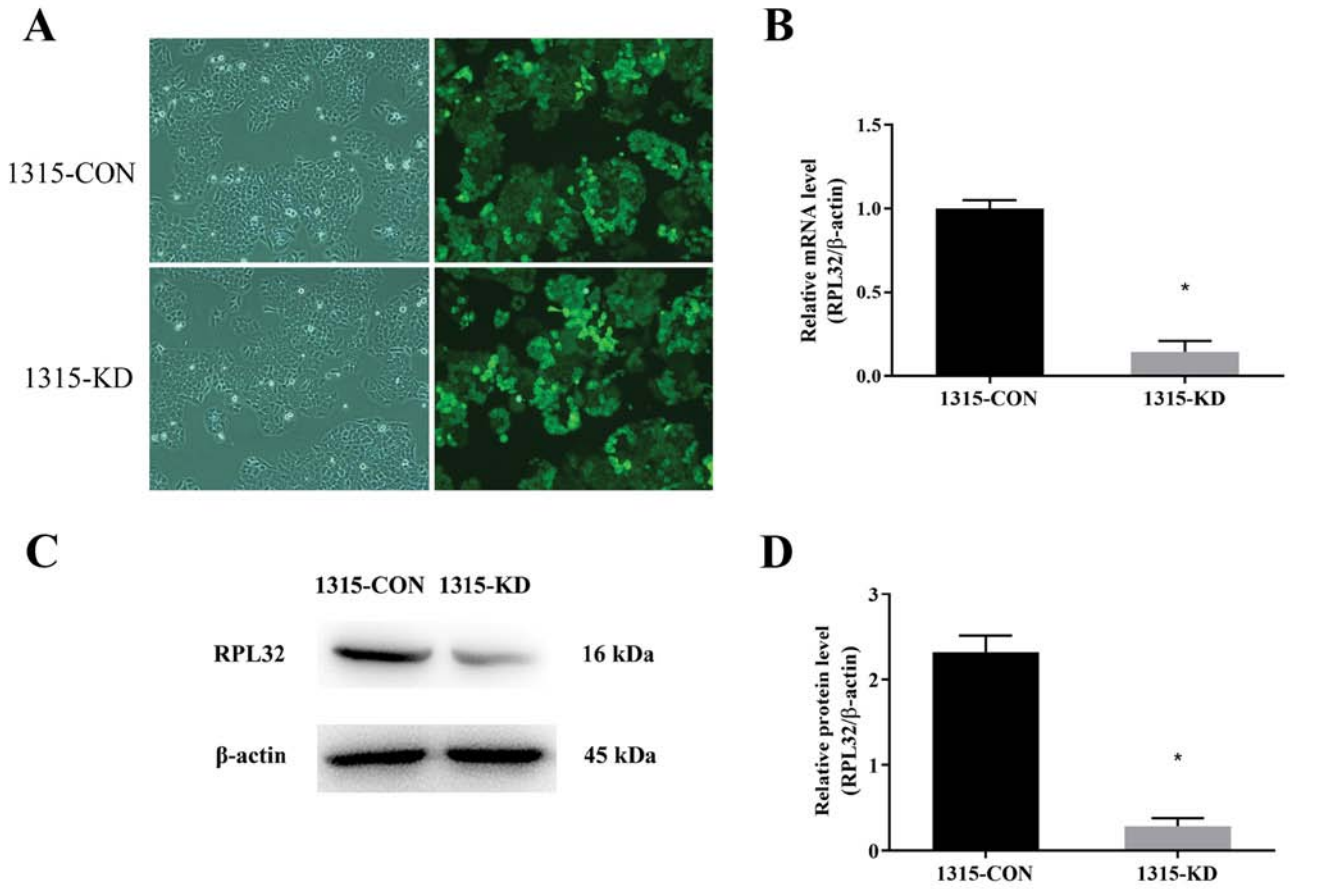

Figure 2. Lentivirus-delivered siRNA silencing specifically inhibits the expression of RPL32 at the mRNA and protein levels. (A) Infection efficiency of the lentivirus was monitored by detecting GFP expression after 3 days of transduction (magnification, x100). (B) Reverse transcription-quantitative PCR demonstrated that the RPL32 mRNA expression was significantly decreased in 1315-KD cells. (C) Western blot analysis identified that (D) RPL32 protein expression was significantly decreased in 1315-KD cells. 1315-CON and SUM 1315 cells were stably transfected with negative control lentivirus, while 1315-KD and SUM 1315 cells were stably transfected with RPL32 siRNA lentivirus. *P<0.05 vs. 1315-CON. si, small interfering; RPL32, ribosomal protein L32; GFP, green fluorescent protein; CON, control; KD, knockdown.

was also significantly decreased by siRNA treatment (Fig. 2C and D); the expression of RPL32 in the 1315-KD group was ~45% of that in the 1315-CON group. These results indicated that lentivirus-delivered siRNA silencing specifically inhibited the expression of RPL32 at the mRNA and protein levels.

Knockdown of RPL32 inhibits migration and invasion of SUM 1315 cells. A CCK-8 assay was performed and 1315-KD cells did not show any difference in proliferation compared with 1315-CON cells. This indicated that RPL32 had no impact on *in vitro* cell proliferation (Fig. 3A). To assess whether RPL32 silencing influenced cell migration and invasion, wound-healing and Transwell assays were performed using SUM 1315 cells. 1315-KD cells exhibited a delayed wound closure of scratch gaps after 24 h (Fig. 3B and C). Transwell assays demonstrated a reduced invasive ability of RPL32-silenced SUM 1315 cells. Moreover, fewer 1315-KD cells invaded the filter, with or without Matrigel, compared with 1315-CON cells (Fig. 3D and E). These data suggested that RPL32 knockdown inhibited the migration and invasion of SUM 1315 cells.

Knockdown of RPL32 decreases the expression levels of MMP-2 and MMP-9. To investigate the molecular mechanisms via which RPL32 silencing inhibits SUM 1315 cell migration and invasion, western blot analysis was performed to detect the expression levels of MMP-2 and MMP-9 (Fig. 4A). The data identified that the expression levels of MMP-9 and MMP-2 was decreased by ~30 and 40%, respectively (Fig. 4B). Thus, it was indicated that RPL32 may promote SUM 1315 cell migration and invasion via the MMP signaling pathway.

RPL32 knockdown suppresses SUM 1315 cell metastasis in vivo. To examine the *in vitro* observations *in vivo*, BC mouse xenografts were generated using 1315-CON and 1315-KD cells. All mice were healthy prior to tumor cell injection. Then, 28 days after cell injection, all xenograft tumors were measured and resected (Fig. 5A). The results demonstrated that the maximum tumor diameter was 14.9 mm and the weight was 1.7 g (9.1% body weight). The maximum percentage of weight loss in the study was 18.5%. There was no significant difference in tumor volume between the 1315-CON and 1315-KD groups (Fig. 5B).

To evaluate the effect of RPL32 on BC tumor metastasis *in vivo*, lung and liver tissues were removed from all xenograft mice. Histological analysis of the lungs identified less metastases in the 1315-KD compared with the 1315-CON group. It was found that 5/9 (55.56%) mice developed lung metastasis

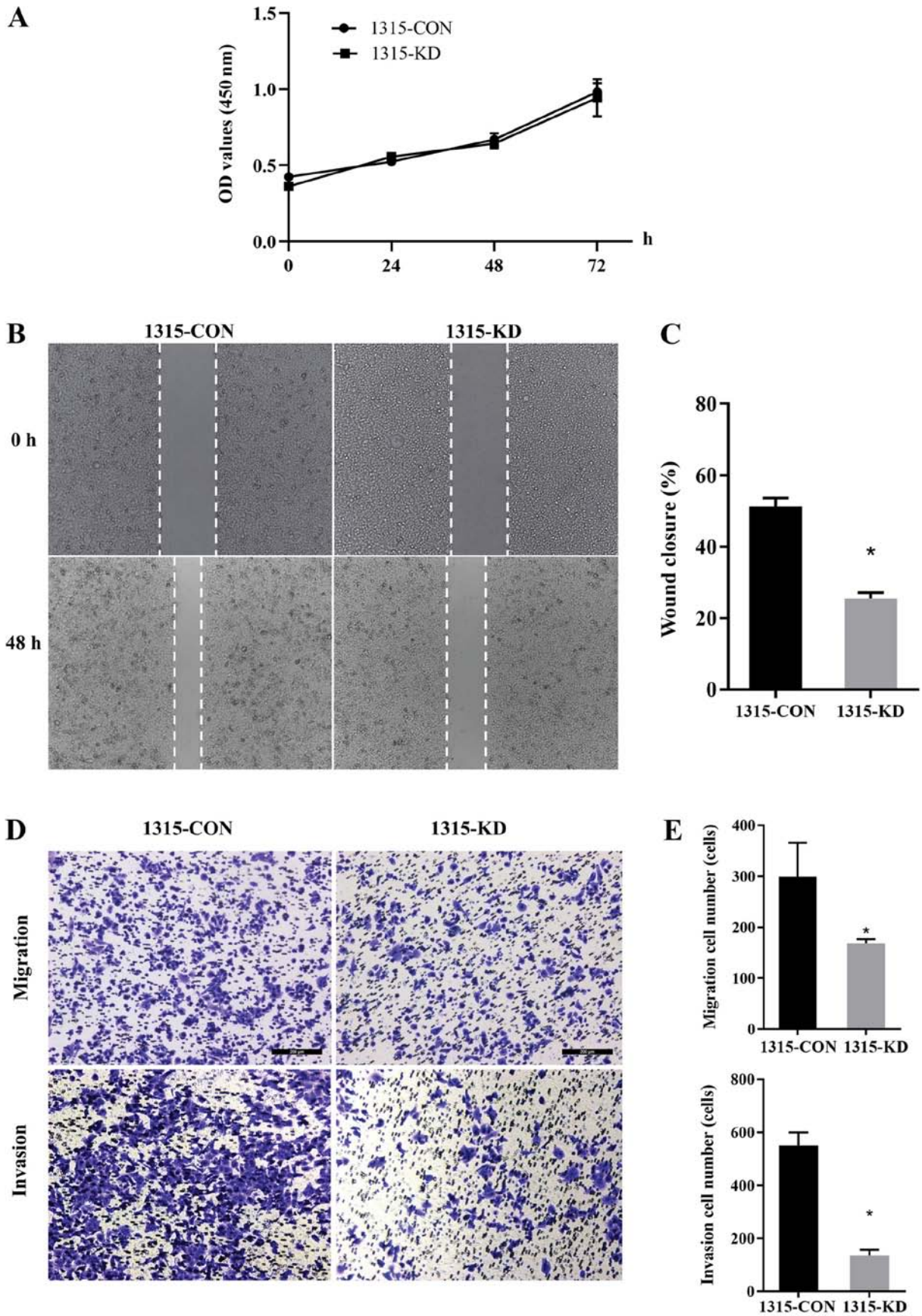

Figure 3. RPL32 knockdown inhibits the migration and invasion of SUM 1315 cells. (A) Cell Counting Kit-8 assay indicated that 1315-KD cells had a similar proliferative ability compared with 1315-CON cells. (B) Wound-healing assay (magnification, x100) demonstrated that RPL32-silenced cells (C) exhibited a delayed wound closure of scratch gaps, compared with the control cells. (D) Transwell assays revealed that (E) fewer 1315-KD cells than 1315-CON cells invaded the filter, with or without Matrigel. 1315-CON and SUM 1315 cells were stably transfected with negative control lentivirus. 1315-KD and SUM 1315 cells were stably transfected with RPL32 siRNA lentivirus. Scale bar, 200 μm. *P<0.05 vs. 1315-CON cells. RPL32, ribosomal protein L32; si, small interfering; CON, control; OD, optical density; KD, knockdown.

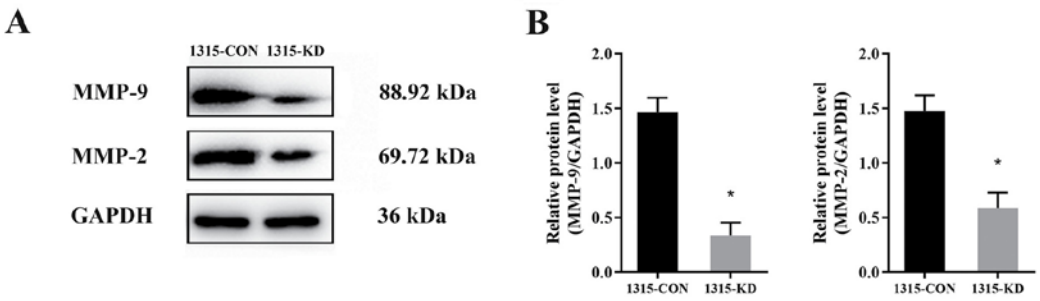

Figure 4. RPL32 knockdown decreases the expression levels of MMP-2 and MMP-9. (A) Western blot analysis indicated that the (B) protein expression levels of both MMP-9 and MMP-2 were lower in 1315-KD cells compared with 1315-CON cells. 1315-CON and SUM 1315 cells were stably transfected with negative control lentivirus. 1315-KD and SUM 1315 cells were stably transfected with RPL32 siRNA lentivirus. *P<0.05 vs. 1315-CON. RPL32, ribosomal protein L32; MMP, matrix metalloproteinase; si, small interfering; CON, control; KD, knockdown.

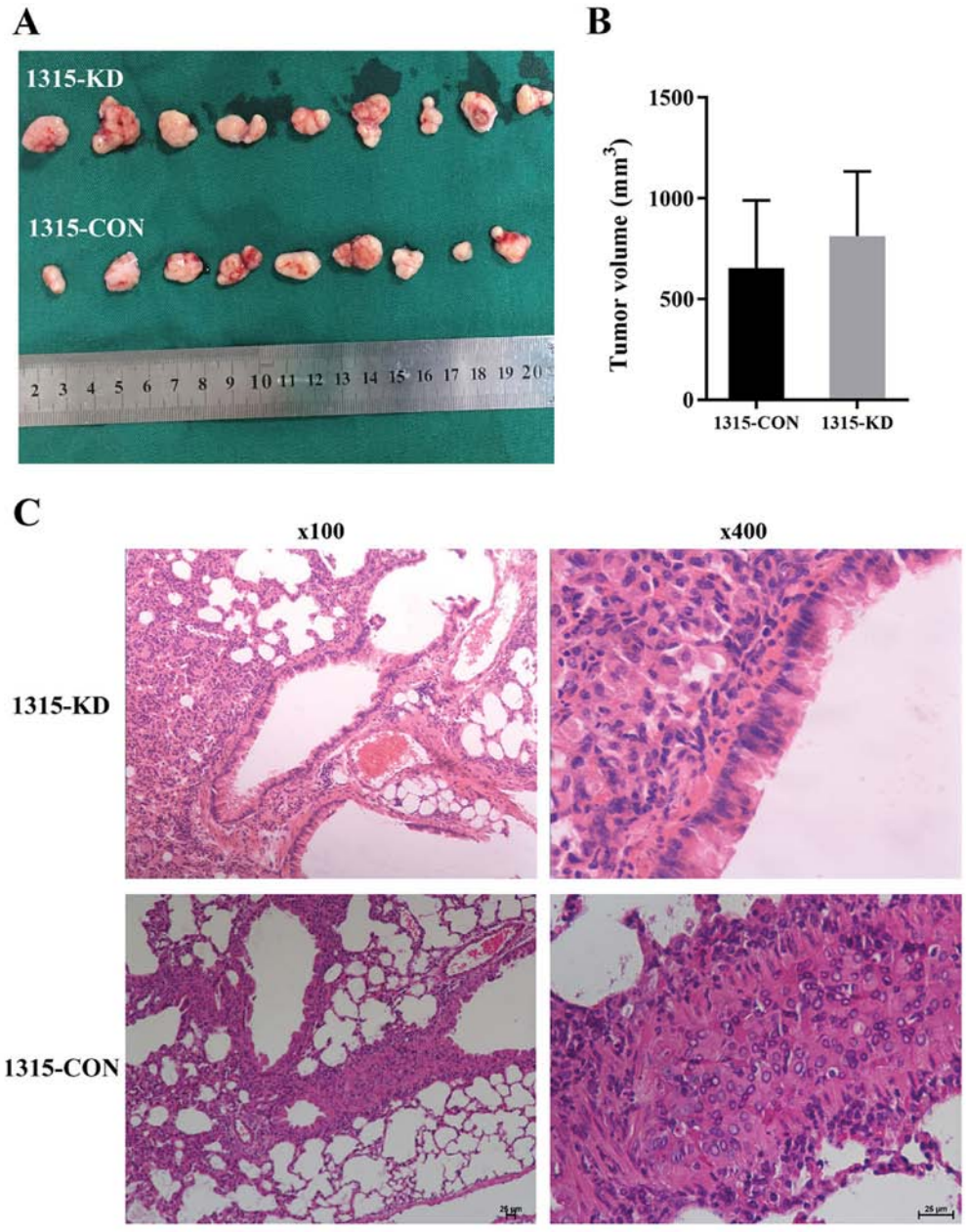

Figure 5. RPL32 knockdown suppresses SUM 1315 cell metastasis *in vivo*. (A) Images of the xenograft tumors were captured at the end of the experiment. (B) Results demonstrated that there was no significant difference in tumor size between the 1315-CON and 1315-KD groups. (C) Histological analysis identified more lung metastases in the 1315-CON compared with the 1315-KD group (magnification at x100 and x400). 1315-CON and SUM 1315 cells were stably transfected with negative control lentivirus. 1315-KD and SUM 1315 cells were stably transfected with RPL32 siRNA lentivirus. RPL32, ribosomal protein L32; si, small interfering; CON, control; KD, knockdown.

in the 1315-CON group, while no (0%) mice developed lung metastasis in the 1315-KD group (Fig. 5C). Furthermore, no liver metastasis was detected in either group (data not shown). Collectively, these data suggested that RPL32 silencing could effectively suppress BC metastasis *in vivo*.

Discussion

Thus far, several RPs have been reported to be associated with certain types of cancer, including cancer of the brain, pancreas and bladder (11-17). However, to the best of our knowledge, few studies have focused on RPs in BC. Previous studies have revealed the oncogenic activity of RPs in BC. For instance, it has been shown that the oncogenic role of RPL39 may be mediated via inducible nitric oxide synthase (22). Another study reported that the overexpression of RPL19 could sensitize BC cells to endoplasmic reticulum stress-induced cell death by activating the unfolded protein response (23). Moreover, a DNA microarray experiment demonstrated that the expression of RPL32, a 60S RP, was correlated with non-small cell lung and prostate cancer types (24,25). However, the role of RPL32 in BC remains to be elucidated.

In the present study, it was found that the RPL32 expression was increased in BC tissues compared with healthy tissues. In addition, RPL32 expression was higher in BC cell lines compared with normal breast epithelial cell line. These results indicated that RPL32 may be associated with BC. Thus, it was hypothesized that RPL32 may serve an important role in BC tumorigenesis.

On the basis of the present findings, a lentivirus carrying an RPL32 siRNA was used to silence the expression of RPL32. Wound-healing assays demonstrated that RPL32-silenced cells exhibited a delayed wound closure of scratch gaps compared with the control cells. In addition, RPL32 silencing significantly reduced the invasion ability of the cells. These results suggested an oncogenic effect of RPL32 on cell migration and invasion in BC. However, no difference in cell proliferation was identified between the groups.

To further examine the underlying mechanism of the RPL32-mediated promotion of cell migration and invasion, western blot analysis was performed to detect MMPs that are associated with cancer cell migration and invasion. Moreover, compared with control cells, the expression levels of MMP-2 and MMP-9 in RPL32-silenced cells were significantly decreased. Thus, these results indicated that RPL32 may decrease BC cell migration and invasion by downregulating MMP expression.

To assess the results *in vivo*, a mouse BC model was constructed. The estimated effect size and level of variability were used to determine the required sample size for future studies. Considering this fact, as well as with the desire to reduce the use of animals, 18 mice were used. 1315-CON and 1315-KD cells were injected into the mammary fat pad of 4-5-week-old nude mice. Then, 28 days later, the tumors were resected and lung and liver tissues were collected. The primary breast tumor volumes were compared between mouse models. No difference was observed between the 1315-CON and 1315-KD mouse groups. This *in vivo* result was consistent with the previous *in vitro* result, which indicated that RPL32 was not associated with tumor proliferation. However, histological analysis demonstrated that cancer cells could be found in lung tissues from the 1315-CON group. In contrast, no cancer cells were identified in lung tissues from the 1315-KD group and no cancer cells were found in liver tissues from both groups. These results indicated that RPL32 silencing could significantly reduce cancer cell metastasis, thus suggesting that RPL32 may be a novel molecular diagnostic target for BC. However, the key molecular mechanism via which RPL32 affects the occurrence and development of BC remains to be elucidated. Moreover, it should be noted that the present study has some limitations. First, only one breast cancer cell line was tested and data of RPL32 upregulation was lacking. Second, the underlying mechanism still needs to be further investigated. In addition, the clinical application of RPL32 marker requires a clinical study.

To the best of our knowledge, the present study was the first to demonstrate the oncogenic function of RPL32 in BC. The molecular mechanism underlying the effect of RPL32 on cell migration and invasion in BC was also preliminarily evaluated. Collectively, it was concluded that PRL32 was a potential target for molecular targeted treatment of BC.

Acknowledgements

Not applicable.

Funding

This research was supported in part by the National Natural Science Foundation of China (grant no. 81302305), Natural Science Foundation of Jiangsu Province (grant no. BK20131027), Jiangsu Province Six Talents Summit Project (grant no. WSW-001), Youth Talent Project (grant no. FRC201308) and a project funded by the Priority Academic Program Development of Jiangsu Higher Education Institutions (grant no. PAPD 0271).

Availability of data and materials

The datasets used and/or analyzed during the current study are available from the corresponding author on reasonable request.

Authors' contributions

JW, SW and LW participated in the study design. LX, CJ, QZ and RC contributed to data collection and analysis. All authors were involved in the writing of the article. JW critically reviewed the manuscript. All authors read and approved the final manuscript.

Ethics approval and consent to participate

All participants provided written informed consent prior to participating in the study. The Institutional Animal Care and Use Committee of Nanjing Medical University approved all the tests conducted in this paper (approval no. IACUC-1706010) and animal procedures were conducted in accordance with the ethical standards in the 1964 Helsinki Declaration. This study was approved by the Ethics and Research Committee of

The First Affiliated Hospital of Nanjing Medical University (approval no. 2013-SRFA-108).

Patient consent for publication

Not applicable.

Competing interests

The authors declare that they have no competing interests.

References

1. McGuire S: World cancer report 2014. Geneva, Switzerland: World Health Organization, International Agency for Research on cancer, WHO Press, 2015. Adv Nutr 7: 418-419, 2016.
2. Song QK, Li J, Huang R, Fan JH, Zheng RS, Zhang BN, Zhang B, Tang ZH, Xie XM, Yang HJ, *et al*: Age of diagnosis of breast cancer in China: Almost 10 years earlier than in the United States and the European Union. Asian Pac J Cancer Prev 15: 10021-10025, 2014.
3. Song QK, Wang XL, Zhou XN, Yang HB, Li YC, Wu JP, Ren J and Lyerly HK: Breast cancer challenges and screening in China: Lessons from current registry data and population screening studies. Oncologist 20: 773-779, 2015.
4. Gray J and Druker B: Genomics: The breast cancer landscape. Nature 486: 328-329, 2012.
5. Ban KA and Godellas CV: Epidemiology of breast cancer. Surg Oncol Clin N Am 23: 409-422, 2014.
6. Wang J, Xia TS, Liu XA, Ding Q, Du Q, Yin H and Wang S: A novel orthotopic and metastatic mouse model of breast cancer in human mammary microenvironment. Breast Cancer Res Treat 120: 337-344, 2010.
7. Zheng MJ, Wang J, Xu L, Zha XM, Zhao Y, Ling LJ and Wang S: Human mammary microenvironment better regulates the biology of human breast cancer in humanized mouse model. Med Oncol 32: 427, 2015.
8. Zheng M, Wang J, Ling L, Xue D, Wang S and Zhao Y: Screening and analysis of breast cancer genes regulated by the human mammary microenvironment in a humanized mouse model. Oncol Lett 12: 5261-5268, 2016.
9. Fatica A and Tollervey D: Making ribosomes. Curr Opin Cell Biol 14: 313-318, 2002.
10. Xue S and Barna M: Specialized ribosomes: A new frontier in gene regulation and organismal biology. Nat Rev Mol Cell Biol 13: 355-369, 2012.
11. Yong WH, Shabihkhani M, Telesca D, Yang S, Tso JL, Menjivar JC, Wei B, Lucey GM, Mareninov S, Chen Z, *et al*: Ribosomal proteins RPS11 and RPS20, two stress-response markers of glioblastoma stem cells, are novel predictors of poor prognosis in glioblastoma patients. PLoS One 10: e0141334, 2015.
12. Shi C, Wang Y, Guo Y, Chen Y and Liu N: Cooperative down-regulation of ribosomal protein L10 and NF-κB signaling pathway is responsible for the anti-proliferative effects by DMAPT in pancreatic cancer cells. Oncotarget 8: 35009-35018, 2017.
13. Paquet ÉR, Hovington H, Brisson H, Lacombe C, Larue H, Têtu B, Lacombe L, Fradet Y and Lebel M: Low level of the X-linked ribosomal protein S4 in human urothelial carcinomas is associated with a poor prognosis. Biomark Med 9: 187-197, 2015.
14. Jung Y, Lee S, Choi HS, Kim SN, Lee E, Shin Y, Seo J, Kim B, Jung Y, Kim WK, *et al*: Clinical validation of colorectal cancer biomarkers identified from bioinformatics analysis of public expression data. Clin Cancer Res 17: 700-709, 2011.
15. Russo A, Saide A, Smaldone S, Faraonio R and Russo G: Role of uL3 in multidrug resistance in p53-mutated lung cancer cells. Int J Mol Sci 18: 547, 2017.
16. Fan H, Li J, Jia Y, Wu J, Yuan L, Li M, Wei J and Xu B: Silencing of ribosomal protein L34 (RPL34) inhibits the proliferation and invasion of esophageal cancer cells. Oncol Res 25: 1061-1068, 2017.
17. Sim EU, Chan SL, Ng KL, Lee CW and Narayanan K: Human ribosomal proteins RPeL27, RPeL43, and RPeL41 are upregulated in nasopharyngeal carcinoma cell lines. Dis Markers 2016: 5179594, 2016.
18. Yang M, Sun H, Wang H, Zhang S, Yu X and Zhang L: Down-regulation of ribosomal protein L22 in non-small cell lung cancer. Med Oncol 30: 646, 2013.
19. Maruyama Y, Miyazaki T, Ikeda K, Okumura T, Sato W, Horie-Inoue K, Okamoto K, Takeda S and Inoue S: Short hairpin RNA library-based functional screening identified ribosomal protein L31 that modulates prostate cancer cell growth via p53 pathway. PLoS One 9: e108743, 2014.
20. Chen J, Wei Y, Feng Q, Ren L, He G, Chang W, Zhu D, Yi T, Lin Q, Tang W, *et al*: Ribosomal protein S15A promotes malignant transformation and predicts poor outcome in colorectal cancer through misregulation of p53 signaling pathway. Int J Oncol 48: 1628-1638, 2016.
21. Livak KJ and Schmittgen TD: Analysis of relative gene expression data using real-time quantitative PCR and the 2(-Delta Delta C(T)) method. Methods 25: 402-408, 2001.
22. Bisaccia F, De Palma A and Palmieri F: Identification and purification of the tricarboxylate carrier from rat liver mitochondria. Biochim Biophys Acta 977: 171-176, 1989.
23. Hong M, Kim H and Kim I: Ribosomal protein L19 overexpression activates the unfolded protein response and sensitizes MCF7 breast cancer cells to endoplasmic reticulum stress-induced cell death. Biochem Biophys Res Commun 450: 673-678, 2014.
24. Dmitriev AA, Kashuba VI, Haraldson K, Senchenko VN, Pavlova TV, Kudryavtseva AV, Anedchenko EA, Krasnov GS, Pronina IV, Loginov VI, *et al*: Genetic and epigenetic analysis of non-small cell lung cancer with NotI-microarrays. Epigenetics 7: 502-513, 2012.
25. Karan D, Kelly DL, Rizzino A, Lin MF and Batra SK: Expression profile of differentially-regulated genes during progression of androgen-independent growth in human prostate cancer cells. Carcinogenesis 23: 967-975, 2002.